JOURNAL OF AIRCRAFT
Vol. 38, No. 2, March–April 2001

Aeroelastic Characteristics of Double-Swept Isotropic and Composite Wings

Kyo-Nam Koo*
Korea Aerospace Research Institute, Taejon 305-600, Republic of Korea

A new planform of a wing having two sweep angles is proposed to enhance the aeroelastic stability with no loss of the aerodynamic benefits of a swept-forward wing. Aeroelastic analysis is performed with the finite element method to model wing structure and the doublet point method to predict aerodynamic loads. The sweep angle of the inboard wing is varied in this analysis, whereas the outboard wing is swept forward to a preselected amount. The results show that the aeroelastic stability can be drastically enhanced by adjusting the sweep angle of the inboard wing. The effect of the fiber orientation on the aeroelastic stability of the double-swept composite wing is studied, and the proper ply angle is identified to maximize critical speed.

Introduction

THE planform of an aircraft wing has evolved to enhance aircraft performance, speed range, and so on. The typical wing planform of the early aircraft was rectangular or elliptic without any sweep angle. The swept-back wing has been a prototype since it was introduced in Germany during World War II. The Junkers Ju 287 bomber developed during World War II was the first aircraft to employ the swept-forward wing. However, few aircraft with a swept-forward wing have been built because the swept-back metallic wing has a greater divergence speed than a correspondently swept-forward metallic wing.[1]

The reintroduction of the swept-forward wing is mainly a result of Krone using advanced composite materials.[2] He showed that the use of composites could prevent the divergence of the swept-forward wing.[3] The application of the advanced composite materials using aeroelastic tailoring led to the emergence of the X-29 aircraft of Grumman.

Many investigations[1,3–9] were done on the aeroelastic stability of swept-forward composite wings. Their main objective was to study the effect of bending-torsion coupling on the aeroelastic stability according to fiber orientation and stacking sequence. The motivation of this research is the inference that the divergence speed of the swept-forward wing will increase as the sweep angle of inboard wing changes keeping the sweep angle of outboard wing constant. This double-swept wing may have the aerodynamic merit of the swept-forward wing in addition to a high divergence speed.

The objective of this paper is to study the aeroelastic characteristics of the double-swept isotropic and composite wings. The wing is assumed to be plate-like. The finite element method for wing structure and the doublet point method for aerodynamic loads are used to model the general-shaped wing. Numerical results show the effect of the inboard sweep angle for the isotropic angle and the effect of the fiber orientation on flutter and divergence speeds.

Aeroelastic Equations

The aeroelastic equation can be derived using Hamilton's principle

$$\delta \int_{t_1}^{t_2} (T - U)\,\mathrm{d}t + \int_{t_1}^{t_2} \delta W\,\mathrm{d}t = 0 \tag{1}$$

where T is the kinetic energy, U the strain energy, and δW the virtual work done by aerodynamic force.

Received 20 July 1999; revision received 15 May 2000; accepted for publication 10 August 2000.

*Senior Researcher, Aircraft Division; currently Assistant Professor of Aerospace Engineering, School of Transportation Systems Engineering, University of Ulsan, Ulsan 680-749, Republic of Korea; knkoo@kari.re.kr.

Because the wing is assumed to be a plate in the $x-y$ plane, the displacement field is expressed using the transverse shear deformable plate theory[10] as

$$u(x, y, z; t) = u_0(x, y; t) + z\phi_x(x, y; t)$$

$$v(x, y, z; t) = v_0(x, y; t) + z\phi_y(x, y; t)$$

$$w(x, y; t) = w(x, y; t) \tag{2}$$

where u, v, and w are the displacements in the x, y, and z directions, respectively; the subscript 0 means the values in the plate midplane; ϕ_x and ϕ_y are the rotations about the y and x axes, respectively.

After expressing T, U, and δW in the displacements in Eq. (2) and applying the constitutive equation relating resultants with strains, the finite element formulation can be achieved through the use of the linear Lagrangian interpolation functions

$$\boldsymbol{M}\ddot{\boldsymbol{u}} + \boldsymbol{K}\boldsymbol{u} = \boldsymbol{f} \tag{3}$$

where $\boldsymbol{M}$ is the mass matrix, $\boldsymbol{K}$ the stiffness matrix, $\boldsymbol{f}$ the force vector, and $\boldsymbol{u}$ the displacement vector consisting of w, ϕ_x, and ϕ_y.

The accurate evaluation of aerodynamic loads is of importance in aeroelastic analysis. Ueda and Dowell[11] developed a simple method for the unsteady aerodynamics described as the doublet point method (DPM), which calculates the steady-state part with no aid of the vortex lattice method.

The pressure coefficient ΔP and the nondimensional upwash velocity $\bar{w}$ on the oscillatory lifting surfaces are related by the following integral equation:

$$\bar{w}(x, y) = \frac{1}{8\pi} \iint_S \Delta P(\xi, \eta) K(x - \xi, y - \eta; k)\,\mathrm{d}\xi\,\mathrm{d}\eta \tag{4}$$

where the kernel $K(x - \xi, y - \eta; k)$ is a function of the reduced frequency k and found in Ref. 11. Dividing the wing planform into element surfaces and allocating a doublet point (ξ_i, η_i) and an upwash point (x_i, y_i) in each element according to the $\frac{1}{4}$–$\frac{3}{4}$ chord rule, Eq. (4) can be discretized into the linear algebraic equation relating the nondimensional upwash vector $\bar{\boldsymbol{w}}$ and the pressure vector $\boldsymbol{p}$ as

$$\bar{\boldsymbol{w}} = \left(2/\rho_\infty V^2\right)\bar{\boldsymbol{A}}(k)\boldsymbol{p} \tag{5}$$

where ρ_∞ is the air density and $\bar{\boldsymbol{A}}(k)$ the matrix of aerodynamic influence coefficients.

The force vector $\boldsymbol{f}^k$ acting on the doublet point can be expressed using Eq. (5) as

$$\boldsymbol{f}^k = \tfrac{1}{2}\rho_\infty V^2 \boldsymbol{S}\bar{\boldsymbol{A}}^{-1}(k)\boldsymbol{D}\boldsymbol{u}^k \tag{6}$$

in which $\boldsymbol{S}$ is the matrix of the aerodynamic element area, $\bar{\boldsymbol{A}}^{-1}(k)$ the inverse of $\bar{\boldsymbol{A}}(k)$, and $\boldsymbol{D}$ the matrix relating the upwash velocity $\bar{\boldsymbol{w}}$ to the wing displacement $\boldsymbol{u}^k$ at the doublet and upwash points.

The force vector acting on the structural grid points is obtained from the $\boldsymbol{f}^k$ in Eq. (6) through the interpolation using the surface spline method[12] as

$$\boldsymbol{f} = \omega^2 \boldsymbol{Q}(k)\boldsymbol{u} \tag{7}$$

where ω is the angular frequency and the aerodynamic matrix is given by

$$\boldsymbol{Q}(k) = \left(\rho_\infty b^2 / 2k\right)\boldsymbol{G}^T \boldsymbol{S}\bar{\boldsymbol{A}}^{-1}(k)\boldsymbol{D}\boldsymbol{G} \tag{8}$$

and $\boldsymbol{G}$ is the interpolation matrix and $\boldsymbol{G}^T$ its transpose matrix to give $\boldsymbol{u}^k = \boldsymbol{G}\boldsymbol{u}$ and $\boldsymbol{f} = \boldsymbol{G}^T\boldsymbol{f}^k$.

The aeroelastic equation can be obtained by substituting Eq. (7) into Eq. (2) as

$$\boldsymbol{M}\ddot{\boldsymbol{u}} + \boldsymbol{K}\boldsymbol{u} - \omega^2 \boldsymbol{Q}(k)\boldsymbol{u} = 0 \tag{9}$$

Because the aerodynamic matrix $\boldsymbol{Q}(k)$ is obtained under the assumption that the lifting surface undergoes harmonic motion, the aeroelastic equation can be expressed as

$$[\boldsymbol{M} + \boldsymbol{Q}(k) - Z\boldsymbol{K}]\boldsymbol{u} = 0 \tag{10}$$

where Z is the complex eigenvalue and the structural damping g is introduced to solve Eq. (10) as follows:

$$Z = (1 + ig)/\omega^2 \tag{11}$$

Using the modal approach through modal transformation $\boldsymbol{u} = \Phi\boldsymbol{q}$ to save computation time, Eq. (10) becomes

$$\Phi^T[\boldsymbol{M} + \boldsymbol{Q}(k) - Z\boldsymbol{K}]\Phi\boldsymbol{q} = 0 \tag{12}$$

where Φ is the modal matrix consisting of N eigenvectors from free vibration analysis. After the complex eigenvalues of Eq. (12) are found for each reduced frequency, the frequency, the structural damping, and the velocity can be obtained as follows:

$$\omega = 1/\sqrt{\mathrm{Re}(Z)}, \qquad g = \mathrm{Im}(Z)/\mathrm{Re}(Z), \qquad V = \omega b/k \tag{13}$$

where Re( ) and Im( ) denote the real and imaginary parts of a variable, respectively; b is the semichord at the wing root. Flutter occurs when the g value intersects the zero axis.

Because the divergence is a static phenomenon, the divergence speed can be computed by neglecting the mass matrix $\boldsymbol{M}$ and applying steady air load by making the reduced frequency k go to zero as

$$\Phi^T\left[\boldsymbol{K} - \tfrac{1}{2}\rho_\infty V^2 \lim_{k\to 0} \boldsymbol{Q}(k)\right]\Phi\boldsymbol{q} = 0 \tag{14}$$

Isotropic Wings

The geometrical definition of the double-swept wing is shown in Fig. 1, in which Λ_i and Λ_o are the sweep angles of the inboard and outboard wings at the centerline, respectively; λ_i and λ_o are the taper ratios; ℓ_i and ℓ_o are the span lengths; and c is the chord length at the root. The sweep angle is considered positive in the aft direction and negative in the forward direction. The structural characteristics for this wing are

$$E = 73.8\ \mathrm{GPa}, \qquad G = 27.6\ \mathrm{GPa}$$
$$t = 1.0\ \mathrm{mm}, \qquad \rho = 2768\ \mathrm{Kg/m^3} \tag{15}$$

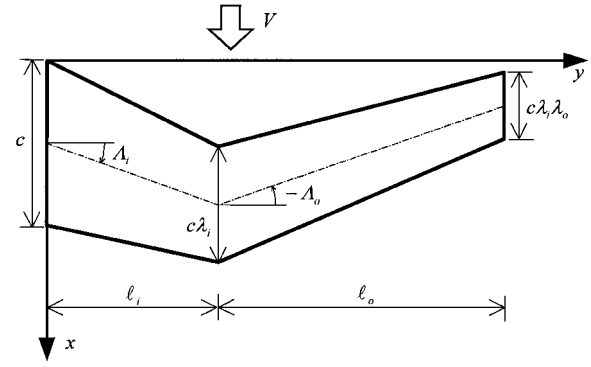

Fig. 1 Geometrical definition and coordinate of double-swept wing.

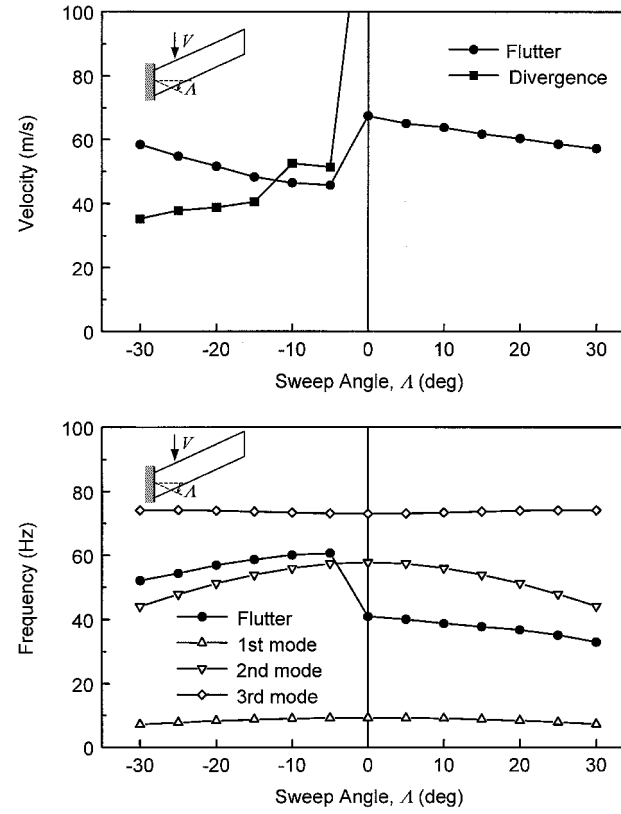

Fig. 2 Flutter and divergence speeds of single-swept isotropic wing vs sweep angle Λ.

Single-Swept Wing

In general, the flutter speed is higher than the divergence speed in case of swept-forward wings and vice versa in case of swept-back wings.[13] This phenomenon is dependent on the relationship between aerodynamic center, elastic center, and center of gravity of wings. The flutter and divergence speeds of straight wings are calculated with a single-sweep angle variation to compare the results with the aeroelastic characteristics of double-swept wings. The geometrical properties of the single-swept wing are

$$c = 76\ \mathrm{mm}, \qquad \ell = \ell_i + \ell_o = 305\ \mathrm{mm}, \qquad \lambda_i = \lambda_o = 1$$
$$\Lambda = \Lambda_i = \Lambda_o = -30\,\mathrm{deg} \sim 30\,\mathrm{deg} \tag{16}$$

The wing structure is modeled with the four-node finite elements. Six finite elements are used in chordwise direction and 16 elements in spanwise direction. The same number of the doublet point elements is used to predict aerodynamic load. The first 10 modes are selected in this aeroelastic analysis. The accuracy of the computational results can be referred to Ref. 9.

Figure 2 shows the influence of sweep angle upon the aeroelastic characteristics of the single-swept wing. The divergence speed

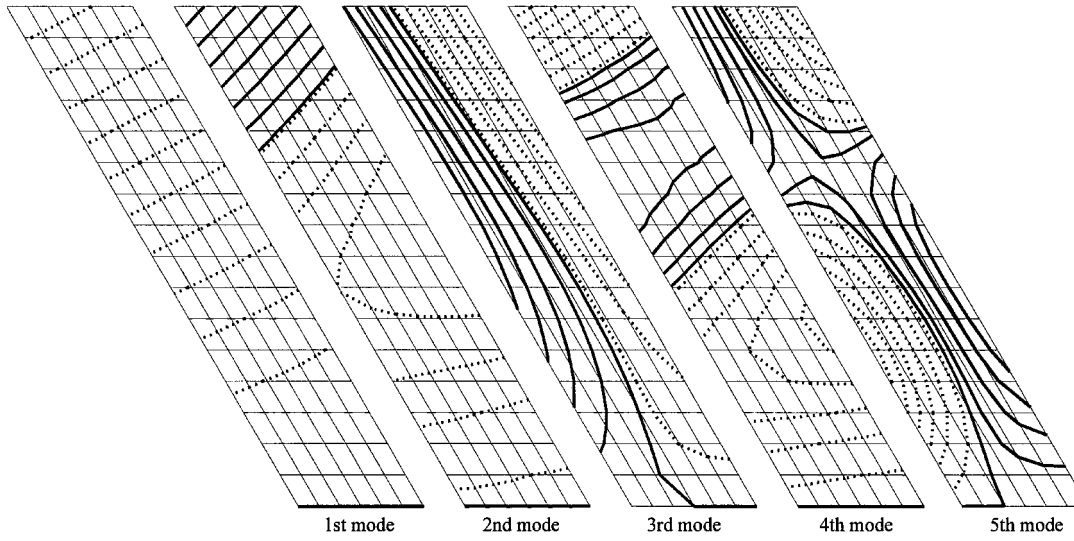

Fig. 3 Mode shapes of single-swept isotropic wing: $\Lambda = -30$ deg.

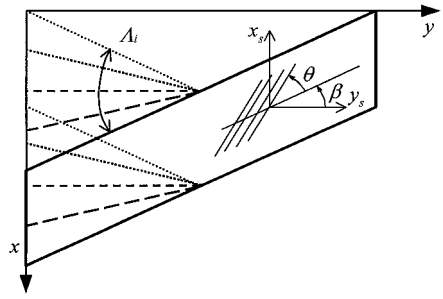

Fig. 4 Variation in sweep angle of inboard wing and definition of fiber orientation.

increases as the sweep angle increases in the aft direction. The flutter speed decreases monotonically, jumps up near $\Lambda = 0$ deg, and then decreases as the sweep angle increases in the aft direction. The reason the flutter speed does not decrease monotonically is that the flutter mode is influenced mainly by the second and third modes in swept-forward wing and mainly by the first and second modes in swept-back one, as shown in Fig. 2.

The mode shapes of free vibration are shown in Fig. 3 for the isotropic single-swept wing with $\Lambda = -30$ deg. The mode shapes of the forward-swept wing are in a wash-in condition, which generally gives a low divergence speed.

Double-Swept Wing

The double-swept wing consists of the inboard and outboard wings with different sweep angles. The swept-forward angle of the outboard wing is held constant to prevent the occurrence of boundary-layer separation or stall at the wing tip, and the inboard sweep angle is varied as shown in Fig. 4 to study the behavior of flutter and divergence instabilities.

Two wings with the different span lengths of an inboard wing are considered to illustrate the effect of the inboard sweep angle on the aeroelastic stability. One wing has a length $\ell_i = 0.25\ell$, whereas the other has a length $\ell_i = 0.5\ell$. The outboard sweep angle remains constant at -30 deg, whereas the inboard sweep angle is varied from -30 to 30 deg. The wing is assumed to have a chord length $c = 76$ mm and a half-span length $\ell = 305$ mm.

Figure 5 shows flutter speed vs Λ_i for $\ell_i = 0.25\ell$ and $\ell_i = 0.5\ell$, and Fig. 6 shows divergence speed vs Λ_i for both lengths. Figure 5 shows that the double-swept wing with $\ell_i = 0.5\ell$ has the maximum flutter speed at $\Lambda_i = 25$ deg, which is about 50% larger than the speed at $\Lambda_i = -30$ deg while the wing with $\ell_i = 0.25\ell$ obtains a small increase of the flutter speed by changing the inboard sweep

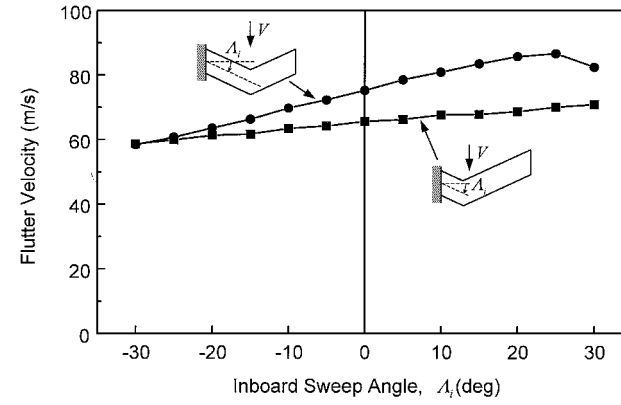

Fig. 5 Flutter speed vs inboard sweep angle Λ_i of double-swept isotropic wing: $\ell_i = 0.25\ell$ and $\ell_i = 0.5\ell$; $\Lambda_o = -30$ deg.

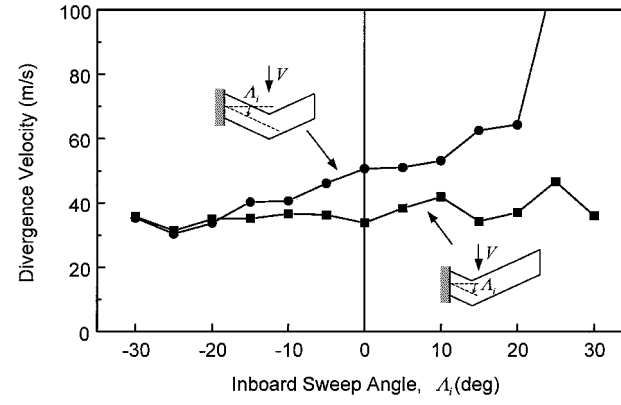

Fig. 6 Divergence speed vs inboard sweep angle Λ_i of double-swept isotropic wing: $\ell_i = 0.25\ell$ and $\ell_i = 0.5\ell$; $\Lambda_o = -30$ deg.

angle. The results in Fig. 6 illustrate that the divergence stability for the double-swept wing can be enhanced by selecting a proper inboard sweep angle. A 30% increase in the divergence speed of the wing with $\ell_i = 0.25\ell$ can be achieved at $\Lambda_i = 25$ deg in comparison with $\Lambda_i = -30$ deg. In the case of $\ell_i = 0.5\ell$, the divergence speed at $\Lambda_i = 25$ deg is about 112.3 m/s, which is three times as large as the speed at $\Lambda_i = -30$ deg. It is observed in Figs. 5 and 6 that the double-swept wing with $\ell_i = \ell_o = 0.5\ell$ can greatly enhance the aeroelastic stability at $\Lambda_i = 25$ deg by increasing the critical speed about 130% larger than the speed of the 30-deg swept-forward wing.

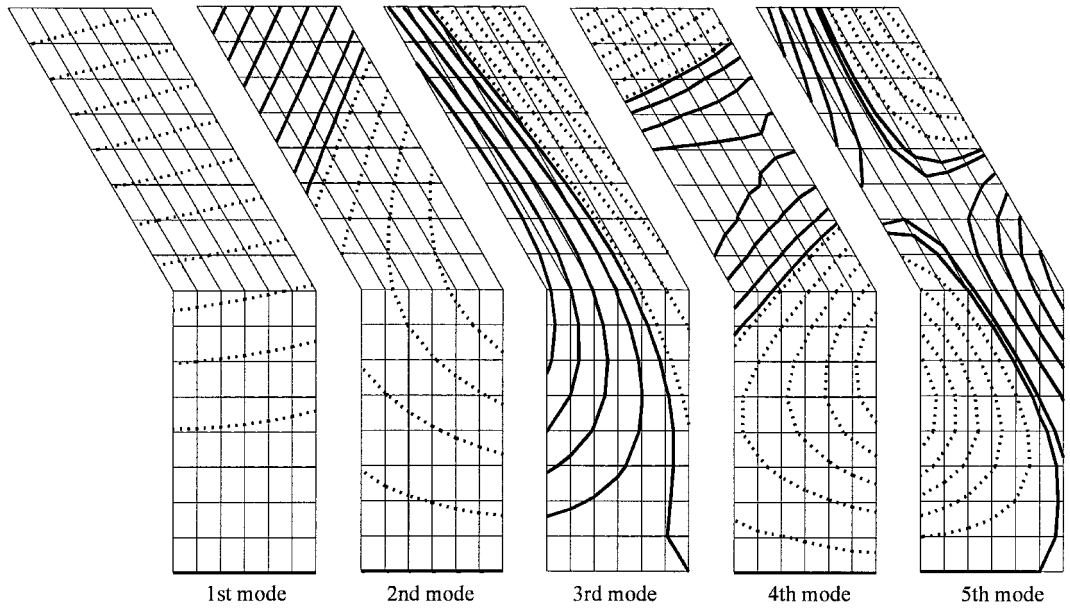

Fig. 7 Mode shapes of double-swept isotropic wing: $\ell_i = 0.5\ell$, $\Lambda_i = 0$ deg, and $\Lambda_o = -30$ deg.

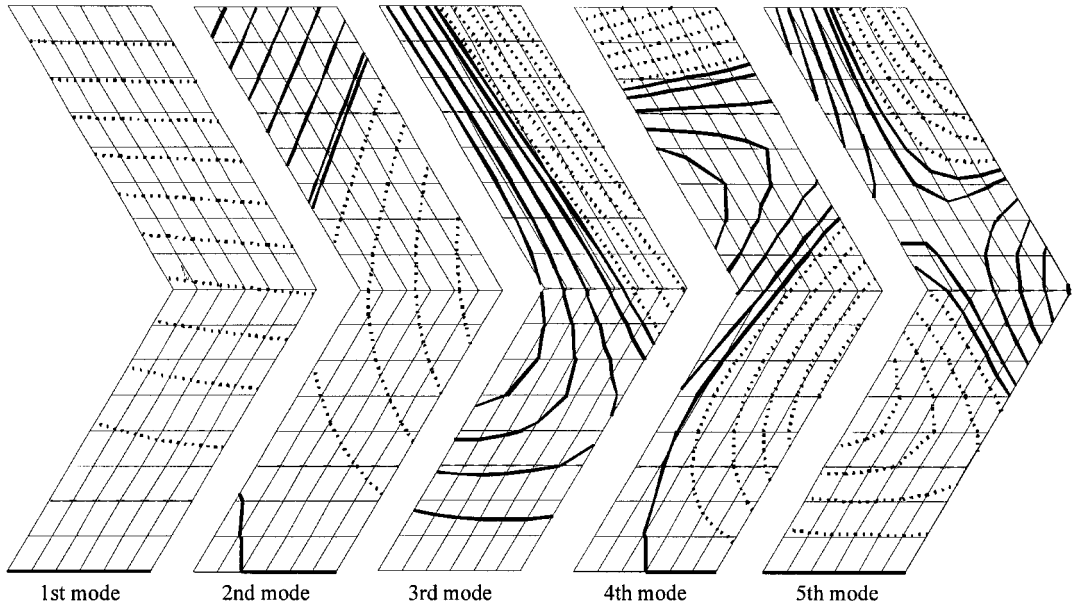

Fig. 8 Mode shapes of double-swept isotropic wing: $\ell_i = 0.5\ell$, $\Lambda_i = 30$ deg, and $\Lambda_o = -30$ deg.

The mode shapes of the double-swept wing for the cases of $\Lambda_i = 0$ and 30 deg are plotted in Figs. 7 and 8, respectively. The contour lines are very similar on the outboard wing for both cases. However, the differences in the deformation pattern on the inboard wing are apparent. The first mode shape for $\Lambda_i = 30$ deg shows wash-in on the inboard wing, whereas that for $\Lambda_i = 0$ deg shows wash-out. In the case of the second mode shape, the wing with $\Lambda_i = 30$ deg has more tendency to wash-in than the wing with $\Lambda_i = 0$.

Composite Wings

Many studies on aeroelastic tailoring have focused on the effect of the bending-torsion coupling of composite material upon the aeroelastic behavior. The stacking sequences considered in those studies are usually made to maximize the bending-torsion coupling. The laminates having such stacking sequences are not used in the aircraft industry where most of composite wings adopt the balanced symmetric laminate consisting mainly of 0-, ±45-, and 90-deg laminae. The composite wings investigated in this study are a quasi-isotropic wing with $[0/\pm 45/90]_S^\beta$ and an anisotropic wing with $[\theta/0/\pm 45/90]_S^\beta$, where β is the reference angle from which the fiber orientation is measured, as shown in Fig. 4. The material data of AS1/3501-6 taken from Ref. 5 are listed next:

$$E_1 = 98.9 \text{ GPa}, \qquad E_2 = 7.9 \text{ GPa}, \qquad G_{12} = 5.6 \text{ GPa}$$
$$\nu_{12} = 0.28, \qquad t = 0.134 \text{ mm}, \qquad \rho = 1520 \text{ Kg/m}^3 \quad (17)$$

Quasi-Isotropic Composite Wing

The aeroelastic characteristics of the quasi-isotropic composite wing are studied for three cases that are discriminated by the reference angle β. The composite wing is double swept at $\ell_i = 0.5\ell$, and the inboard sweep angle Λ_i is varied from -30 to 30 deg with the Λ_o fixed at -30 deg.

Figure 9 shows the effect of the inboard sweep angle on the flutter speed of the composite wing with $[0/\pm 45/90]_S^\beta$. Three reference angles are considered in Figs. 9 and 10: $\beta = -30$, 0, and 30 deg. The

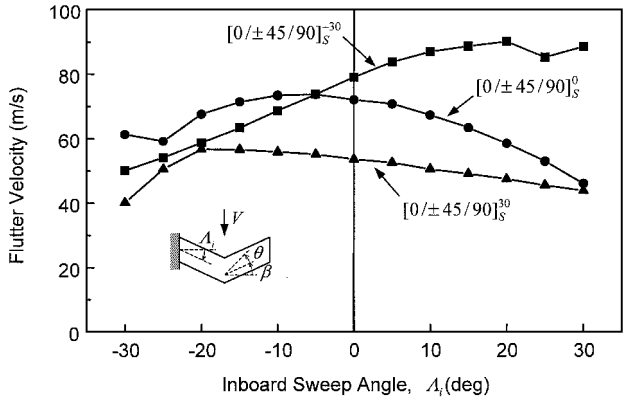

Fig. 9 Flutter speed vs inboard sweep angle Λ_i of double-swept quasi-isotropic wing: $[0/\pm 45/90]_S^{\beta}$, $\ell_i = 0.5\ell$, and $\Lambda_o = -30$ deg.

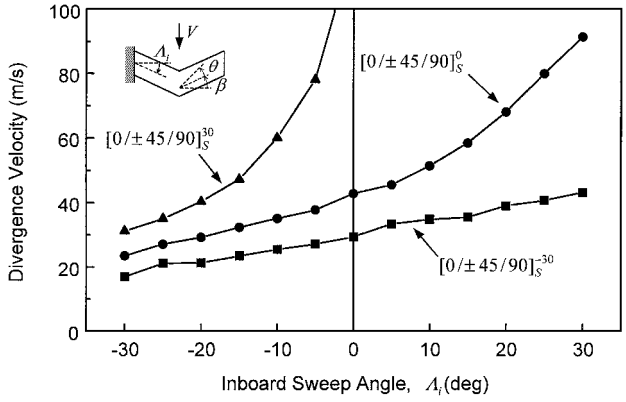

Fig. 10 Divergence speed vs inboard sweep angle Λ_i of double-swept quasi-isotropic wing: $[0/\pm 45/90]_S^{\beta}$, $\ell_i = 0.5\ell$, and $\Lambda_o = -30$ deg.

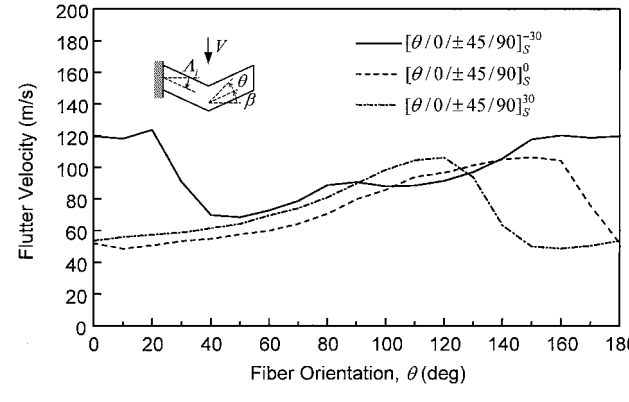

Fig. 11 Effect of fiber orientation on flutter speed of double-swept anisotropic wing: $[\theta/0/\pm 45/90]_S^{\beta}$, $\ell_i = 0.5\ell$, $\Lambda_i = -30$ deg, and $\Lambda_o = -30$ deg.

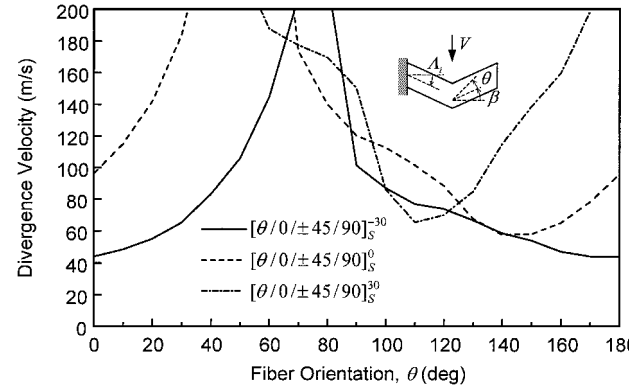

Fig. 12 Effect of fiber orientation on divergence speed of double-swept anisotropic wing: $[\theta/0/\pm 45/90]_S^{\beta}$, $\ell_i = 0.5\ell$, $\Lambda_i = -30$ deg, and $\Lambda_o = -30$ deg.

change in the flutter speed with the inboard sweep angle is strongly dependent on the reference angle β. For $\beta = 0$ and 30 deg the maximum flutter speed occurs in the negative Λ_i. For $\beta = -30$ deg, however, the maximum flutter speed is reached near $\Lambda_i = 20$ deg. It is found in Fig. 9 that the variation of the inboard sweep angle Λ_i can increase the flutter speed.

Figure 10 illustrates the divergence behavior for the three cases. The change in the divergence speed is monotone as Λ_i is increased. Especially, in the case of $\beta = 30$ deg the divergence speed is the highest over the entire range of Λ_i.

From the results in Figs. 9 and 10, it is found that the maximum flutter speed can be obtained in the case of $\beta = -30$ deg whereas the maximum divergence speed is in the case of $\beta = 30$ deg. However, the wing with $\beta = 0$ deg has the maximum unstable speed (61.7 m/s) at $\Lambda_i = 16.7$ deg. It means that a proper selection of the reference angle for fiber orientation is of great significance from the viewpoint of the aeroelastic characteristics of double-swept composite wings.

Anisotropic Composite Wing

The double-swept anisotropic wing with the laminate $[\theta/0/\pm 45/90]_S^{\beta}$ is chosen to study the effect of the fiber orientation on the aeroelastic stability. The wing has the geometrical configuration of $\ell_i = 0.5\ell$, $\Lambda_i = 30$ deg, and $\Lambda_o = -30$ deg. The selected reference angles β are 30, 0, and -30 deg as in the case of the quasi-isotropic wing.

Figure 11 illustrates the effect of the fiber orientation θ on the flutter speed of the double-swept anisotropic wing. A complex platform of the double-swept wing makes it difficult to interpret the relationship between fiber orientations and flutter stability. Because a swept-back wing is, in general, more critical to flutter than a swept-forward wing, the fiber orientation in the inboard wing ($0 \le x \le \ell_i$) may play an important role in the aeroelastic instability. The highest flutter speeds in the cases of $\beta = 30$, 0, and -30 deg occur at the fiber orientations $\theta = 120$, 150, and 180 deg, respectively. All of the fiber orientations are 150 deg when it is measured from the y_s axis defined in Fig. 4. Such fiber orientations lead to a wash-in condition in the inboard wing that is swept back. Therefore, it can be said that the wash-in condition in the inboard wing makes the flutter speed highest at the fiber orientation. The wing with $[\theta/0/\pm 45/90]_S^{-30}$ has higher flutter speeds than the others over the entire range. This is because the wing with $[0/\pm 45/90]_S^{-30}$ has much higher flutter speed than the others at $\Lambda_i = 30$ deg, as shown in Fig. 9.

Figure 12 plots the effect of the fiber orientation on the divergence speed of the double-swept wing. The divergence speeds for each case are high when the fiber orientation is set to an angle to give a wash-out condition in the outboard wing. The angles are about 15 deg for $[\theta/0/\pm 45/90]_S^{30}$, 45 deg for $[\theta/0/\pm 45/90]_S^{0}$, and 75 deg for $[\theta/0/\pm 45/90]_S^{-30}$. The range where the divergence speed is high depends on the reference angles β for the fiber orientation. The range where the divergence speed is high is relatively narrow for the case of $[\theta/0/\pm 45/90]_S^{-30}$. This result conforms to the fact that the divergence speed of the quasi-isotropic wing with $[0/\pm 45/90]_S^{-30}$ is relatively low, as shown in Fig. 10. Comparison of Fig. 12 with Fig. 11 shows that the minimum divergence speed occurs when the flutter speed is highest. This phenomenon is the well-known aeroelastic tradeoff in flutter and divergence.

Conclusions

An improvement of aeroelastic stability has been attempted by proposing a double-swept wing, which has two sweep angles. The main idea is to make the inboard sweep angle of a swept-forward wing be swept back to increase the divergence speed with no loss of the aerodynamic advantage of the swept-forward wing. The finite element method and the doublet point method are used to take into account the generic wing shape.

The numerical examples are presented for the isotropic metal, quasi-isotropic, and anisotropic composite wings. It is remarkable that the proposed double-swept isotropic wing greatly increases both the flutter speed and the divergence speed by properly selecting the inboard sweep angle. The effects of the fiber orientation have been studied on the aeroelastic stability of the double-swept composite wing. It can be concluded that the bending-torsion coupling can be utilized to enhance the aeroelastic stability of the double-swept composite wing.

One may well question whether the double-swept wing can lose the aerodynamic benefits of the swept-forward wing. And it should be noted that the double-swept angle may need the structural reinforcement at the root of outboard wing. More research into the fields of aerodynamics, strength, and flight stability will make the double-swept wing be a viable design concept.

References

[1]Weisshaar, T. A., "Divergence of Forward Swept Composite Wings," *Journal of Aircraft*, Vol. 17, No. 7, 1980, pp. 442–448.

[2]Shirk, M. H., Hertz, T. J., and Weisshaar, T. A., "Aeroelastic Tailoring—Theory, Practice, and Promise," *Journal of Aircraft*, Vol. 23, No. 1, 1980, pp. 6–18.

[3]Krone, N. J., Jr., "Divergence Elimination with Advanced Composite," AIAA Paper 75-1009, Aug. 1975.

[4]Weisshaar, T. A., "Aeroelastic Tailoring of Forward Swept Composite Wing," *Journal of Aircraft*, Vol. 18, No. 8, 1981, pp. 669–676.

[5]Hollowell, S. J., and Dugundji, J., "Aeroelastic Flutter and Divergence of Stiffness Coupled, Graphite/Epoxy Cantilevered Plates," *Journal of Aircraft*, Vol. 21, No. 1, 1981, pp. 69–76.

[6]Lansberger, B. J., and Dugundji, J., "Experimental Aeroelastic Behavior of Unswept and Forward-Swept Cantilever Graphite/Epoxy Wings," *Journal of Aircraft*, Vol. 22, No. 8, 1985, pp. 679–686.

[7]Lottati, I., "Flutter and Divergence Aeroelastic Characteristics for Composite Forward Swept Cantilever Wing," *Journal of Aircraft*, Vol. 22, No. 11, 1985, pp. 1001–1007.

[8]Lin, K.-J., Lu, P.-J., and Tarn, J.-Q., "Flutter Analysis of Cantilever Composite Plates in Subsonic Flow," *AIAA Journal*, Vol. 27, No. 8, 1989, pp. 1102–1109.

[9]Koo, K. N., and Lee, I., "Aeroelastic Behavior of a Composite Plate Wing with Structural Damping," *Computers and Structures*, Vol. 50, No. 2, 1994, pp. 167–176.

[10]Yang, P. C., Norris, C. H., and Stavsky, Y., "Elastic Wave Propagation in Heterogeneous Plates," *International Journal of Solids and Structures*, Vol. 2, 1966, pp. 665–684.

[11]Ueda, T., and Dowell, E. H., "A New Solution Method for Lifting Surfaces in Subsonic Flow," *AIAA Journal*, Vol. 20, No. 3, 1982, pp. 348–355.

[12]Harder, R. H., and Desmarais, R. N., "Interpolation Using Surface Spline," *Journal of Aircraft*, Vol. 9, No. 2, 1972, pp. 189–191.

[13]Bisplinghoff, R. L., Ashley, H., and Halfman, R. L., *Aeroelasticity*, Addison Wesley Longman, Reading, MA, 1957, p. 13.